# Activities and Phase Diagram Data of NaF − AlF$_3$ − Al$_2$O$_3$ Mixtures Derived from Electromotive Force and Cryoscopic Measurements. Standard Thermodynamic Data of β-Al$_2$O$_3$(s), Na$_3$AlF$_6$(s), Na$_5$Al$_3$F$_{14}$(s) and NaAlF$_4$(l)

ÅSMUND STERTEN, KJELL HAMBERG and INGE MÆLAND

Institutt for teknisk elektrokjemi, NTH, Univ. i Trondheim, N-7034 Trondheim-NTH, Norway

Activity data of NaF and AlF$_3$ were derived from electromotive force (emf) measurements of various types of galvanic cells containing NaF − AlF$_3$ melts saturated with alumina. The transport number of Na$^+$ increases with increasing content of AlF$_3$ and approaches unity for melts more acidic than the cryolite 3NaF·AlF$_3$ composition. Phase diagram data obtained in conjunction with the emf measurements were in excellent agreement with corresponding cryoscopic data. The standard Gibbs energy change associated with the reaction

$$3NaF(l) + AlF_3(s) = Na_3AlF_6(s)$$
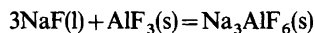
was derived as $\Delta G° = -151.745(\pm 0.550) + 0.0290$ $(\pm 0.0005)T$ kJ (998 K $< T <$ 1237 K) with a standard deviation of ± 0.250 kJ. Corresponding data for the formation of chiolite (Na$_5$Al$_3$F$_{14}$) according to

$$5NaF(l) + 3AlF_3(s) = Na_5Al_3F_{14}(s)$$
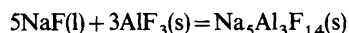
was found to be $\Delta G° = -229.890(\pm 1.290) + 0.00647$ $(\pm 0.00013)T$ kJ (956 K $< T <$ 998 K) with a standard deviation of ± 0.043 kJ. For the reaction

$$NaF(l) + AlF_3(s) = NaAlF_4(l)$$
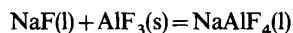
the following expression was obtained, $\Delta G° = 27.167$ $- 0.07283T$ kJ (956 K $< T <$ 1300 K) with an estimated uncertainty of ± 4 kJ. The equilibrium between α-Al$_2$O$_3$ and β-Al$_2$O$_3$ (Na$_2$O·xAl$_2$O$_3$) can be expressed by

$$2NaF(l) + \frac{3x+1}{3}\,\alpha\text{-Al}_2O_3(s) = Na_2O \cdot xAl_2O_3(s)$$
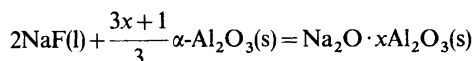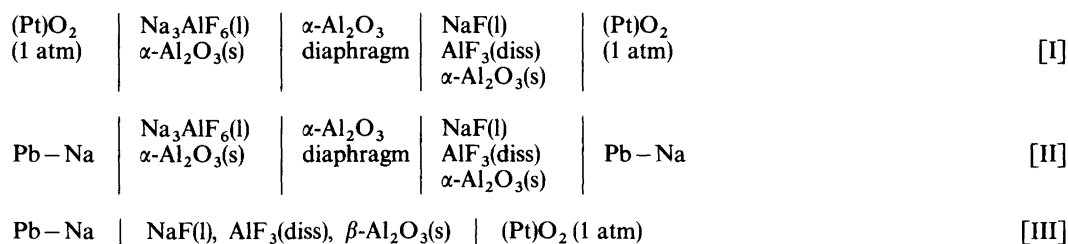
for which the standard Gibbs energy, enthalpy and entropy changes at 1300 K were determined as $\Delta G°$ $= 47.250$ kJ, $\Delta H° = -11.460$ kJ and $\Delta S° = -45.162$ J/degree. The enthalpy and entropy changes of this reaction decrease with decreasing temperature. A discussion of the interaction between aluminium and the melt is also given.

$$6NaF + Al_2O_3 = 2AlF_3 + 3Na_2O \tag{1}$$
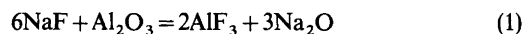
The ternary reciprocal system, eqn. (1), is important from a technical point of view since it constitutes the basic electrolyte in the Hall-Heroult process for the electrolytic production of aluminium. Thermodynamic data for the greater part of the system have not yet been established.[1] The present work was undertaken in order to determine activity data for NaF − AlF$_3$ melts saturated with alumina. Such data are most conveniently derived from emf measurements. In a previous study[2] it was demonstrated that the Pt/O$_2$ electrode behaves reversibly in such melts.

The three cells given in Scheme 1 were applied in the present study. The melt compositions were varied in the right hand side compartments of the concentration cells [I] and [II]. The melts in these cells were always saturated with α-Al$_2$O$_3$, while the NaF − AlF$_3$ melts in cell [III] were saturated with β-Al$_2$O$_3$. The lines separating the stability ranges of α-Al$_2$O$_3$ and β-Al$_2$O$_3$ are illustrated in Fig. 1. Yoshida and Dewing[3] and Thonstad and Rolseth[4] obtained emf data by replacing the oxygen electrodes in cell [II] with aluminium electrodes. This cell was also

4

| (Pt)O$_2$ (1 atm) | Na$_3$AlF$_6$(l) α-Al$_2$O$_3$(s) | α-Al$_2$O$_3$ diaphragm | NaF(l) AlF$_3$(diss) α-Al$_2$O$_3$(s) | (Pt)O$_2$ (1 atm) | [I] |

| Pb−Na | Na$_3$AlF$_6$(l) α-Al$_2$O$_3$(s) | α-Al$_2$O$_3$ diaphragm | NaF(l) AlF$_3$(diss) α-Al$_2$O$_3$(s) | Pb−Na | [II] |

| Pb−Na | NaF(l), AlF$_3$(diss), β-Al$_2$O$_3$(s) | (Pt)O$_2$ (1 atm) | [III] |

Scheme 1.

used in a single run of the present study. The results of these authors[3,4] are discussed in terms of corresponding data from the present work. Some phase diagram data for the ternary reciprocal system (1) are reported and compared with data from the literature. Standard Gibbs energy of formation of β-Al$_2$O$_3$(s), Na$_3$AlF$_6$(s), Na$_5$Al$_3$F$_{14}$(s) and NaAlF$_4$(l) together with enthalpy and entropy values are also derived. Finally, vapour pressures of Na(g) and AlF(g) are calculated as a function of composition for melts in equilibrium with aluminium metal.

The conditions required for the existence of concentration gradients in the diffusion layer on the electrolytic side of the metal−melt interface are discussed.

THEORY

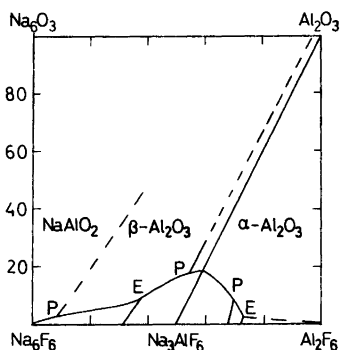Unless specified otherwise, the ternary reciprocal system (1) is taken to be constituted of the

Fig. 1. Schematic diagram of the ternary reciprocal system Na$_6$F$_6$−Al$_2$F$_6$−Al$_2$O$_3$−Na$_6$O$_3$. Some eutectic (E) and peritectic (P) points are indicated together with the corresponding crystallization fields. The diagram is based on data from Foster,[17,18] Holm[19] and the present work.

components NaF, AlF$_3$ and Al$_2$O$_3$.

The α-Al$_2$O$_3$ diaphragm in cells [I] and [II] acts as a semipermeable membrane in cryolite melts saturated with alumina.[2,3] The emf of cell [I] generated between two identical oxygen electrodes is denoted E_1 while the emf of cell [II] with corresponding melt composition is denoted E_2. The corresponding cell reactions contain transport numbers which need not be known in the present case. Subtracting cell reaction [II] from cell reaction [I] cancels these transport numbers. The resulting reaction is given in eqn. (2). The components in the

$$6NaF(l) + 2 AlF_3 + Al_2O_3(l) = 6 NaF + 2 AlF(l) + Al_2O_3 \qquad (2)$$
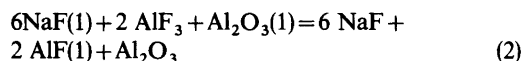
reference compartments on the left hand side of the cells [I] and [III] are denoted (1). The emf corresponding to reaction (2), is as given in eqn. (3),

$$E = E_1 - E_2 = \frac{RT}{F} \ln \left[\frac{a_{NaF(1)}}{a_{NaF}} \right] + \frac{RT}{3F} \ln \left[\frac{a_{AlF_3}}{a_{AlF_3(1)}} \right] \qquad (3)$$

keeping in mind that the melts in both cells are saturated with α-Al$_2$O$_3$, the standard state of the activity. This means also that the Gibbs-Duhem equation can be written as eqn. (4), where r is the mol

$$d \ln a_{AlF_3} = -r \, d \ln a_{NaF} \qquad (4)$$

ratio $n_{NaF} - n_{AlF_3}$. Derivation of eqn. (3) and combining with eqn. (4) yields eqn. (5) or alternatively eqn. (6).

$$d \ln a_{AlF_3} = \frac{3Fr \, dE}{RT(r+3)} \qquad (5)$$

$$\text{d ln}_{NaF} - \frac{3F\,\text{d}E}{RT(r+3)} \tag{6}$$

Graphical integration of eqn. (5) is straightforward since emf measurements are available for melts saturated with AlF$_3$, the standard state of the activity. For, the melt compositions applied we do not have an absolute value for the activity of NaF. The only ions of importance in the basic part of the pure NaF − Na$_3$AlF$_6$ melts are F$^-$ and AlF$_6^{3-}$ with the common cation Na$^+$. It has been shown [5] that the Temkin model [6] is roughly valid in such melts. Thus, the activity of NaF is readily calculated as 0.92 for $r = 15$ ($x_{AlF_3} = 0.0625$). Adding alumina to this melt the temperature of first crystallization decreases slightly,[5] which also means a minor decrease of the activity of NaF. The numerical value of the activity is taken to be 0.90 when the melt becomes saturated with alumina. The error involved in applying this activity value of liquid NaF should be quite small.

The α-Al$_2$O$_3$ diaphragm breaks down rapidly if it is used in basic melts where β-Al$_2$O$_3$ is the stable solid compound. Therefore, cell [III] was applied for melt compositions in the stability range of β-Al$_2$O$_3$. The cell reaction is given in eqn. (7), with the

$$2Na_{(in\ Pb)} + \tfrac{1}{2}O_2(g,\ 1\ atm) = Na_2O(l) \tag{7}$$
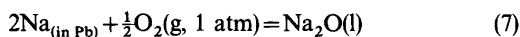
$$E_3 = E_3^{\circ} - \frac{RT}{2F} \ln \left[a_{Na_2O}/a_{Na}^2 \right] \tag{8}$$

$$E_3 = E' - \frac{RT}{3F} \ln \left[a_{NaF}^3/a_{AlF_3} \right] \tag{9}$$

corresponding emf E_3, eqn. (8). Oxygen at 1 atm. pressure was chosen as the standard state. Eqn. (8) is combined with the equation for the equilibrium constant for reaction (1) which gives eqn. (9), where E' is assumed to be a constant for a given temperature and a fixed activity of sodium. This is not strictly correct, since the activity of Al$_2$O$_3$ decreases slightly with increasing basicity in the stability range of β-Al$_2$O$_3$. However, the error in the final activity data caused by this simplified treatment is believed to be negligible.

Derivation of eqn. (9) and combining with eqn. (4) give equations identical with those derived for the cells [I] and [II]. Eqns. (5) and (6) combined with emf data from cell [III] are then used to derive activities in the stability field of β-Al$_2$O$_3$.

EXPERIMENTAL

The melts in the compartments on the right-hand side of cells [I] and [II] were contained in alumina tubes serving as diaphragms between the electrode compartments. The main cell crucible was also made of α-Al$_2$O$_3$.

The oxygen electrode in cell [III] was located inside an open ended α-Al$_2$O$_3$ tube. The electrode and the tube were lowered into the melt only during the emf measurements. The time of immersion was made as short as possible in order to minimize the transformation reaction of α-Al$_2$O$_3$ to β-Al$_2$O$_3$ and to protect the oxygen electrode against possible attack by dissolved metal.[2]

The weighing and the preparation of sodium electrodes were carried out in a dry box. A freshly prepared piece of sodium metal was wrapped in lead foil and placed in a small alumina container. This container was then transferred to the main cell which was a graphite crucible. Electrical contact to the electrode was established by means of a tantalum wire of 1 mm diameter shielded by an alumina tube.

The cryoscopic measurements were carried out by using a mechanical stirrer in a graphite crucible. The Pt − Pt 10Rh thermocouple applied was calibrated several times against the melting point of silver, 1235.1 K. Other details of the cells with accessories are described elsewhere.[2]

The chemicals used were sublimed AlF$_3$, handpicked Greenland cryolite, and reagent grade NaF supplied by Merck.

RESULTS AND DISCUSSION

Emf data. Fig. 2 shows that the emf of cell [II] as a function of r can be fitted to a linear relationship within the limits of experimental uncertainty. It was not possible to obtain reliable emf readings for $r < 2$,
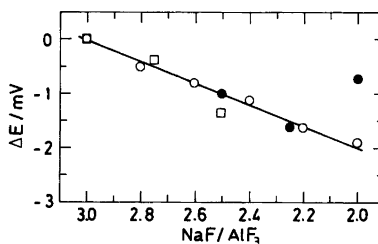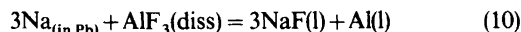

Fig. 2. The variation of the emf of cell [II] with the mol ratio NaF − AlF$_3$ in melts saturated with α-Al$_2$O$_3$ at 1278 K. One symbol for each series of experiments.

probably because a separate aluminium phase was formed according to the reaction (10).

$$3Na_{(in\ Pb)} + AlF_3(diss) = 3NaF(l) + Al(l) \qquad (10)$$

The sodium content of the Na − Pb alloy electrode was in the range 0.5 to 1.0 weight %. As long as the reaction is displaced to the left ($r < 2$) the alloy electrode will contain only minor amounts of aluminium.[8−11]

The variation of only 2 mV in the emf over the compositional range shown in Fig. 2 means that the transport number of Na^+ is close to unity as discussed below. This means also that the Na − Pb alloy acts as a reliable sodium electrode. The variation of the emf with time was usually within ± 0.1 mV/h but occasionally it increased to ± 0.5 mV/h.

Fig. 3 shows emf data of cell [I] as a function of temperature and composition. Within the experimental uncertainties the emf does not change with the temperature in the range of composition shown in the figure. All the points given represent average values from several runs carried out under identical conditions. A reference melt with $r = 1.15$ was also used in several runs in order to establish emf data along the boundary lines shown in the

figure. The data plotted along these univariant curves are based on the assumption of a temperature independent emf for $r = 1.15$ as shown by the solid line in Fig. 3. Accurate and reproducible emf data were obtained with this reference melt when the other cell compartment contained melts in equilibrium with solid AlF_3 and solid α-Al_2O_3. The cooling rate of the cell was never allowed to exceed 1 degree/min during these measurements. However, the temperature of the cell had to be stabilized applying the same reference melt ($r = 1.15$) and melt compositions in the other compartment corresponding to the $Na_3AlF_6(s)$, $Al_2O_3(s)/Al_2O_3(s)$ univariant line, shown in Fig. 3. Phase diagram data to be discussed below show that the emf is independent of temperature for all acidic melt compositions studied in the present work. The single point in Fig. 3, obtained with cell [I] using two aluminium electrodes, is in general agreement with the other data given in the figure. This point is discussed below.

Fig. 4 shows emf data of cell [III] as a function of r at 1278 K. The emf of the reference melt, cryolite saturated with alumina, is taken to be zero. For melt compositions corresponding to $r > 17$ it was not possible to obtain reliable readings since the emf was unstable. Actually, the emf of cell [III] was less
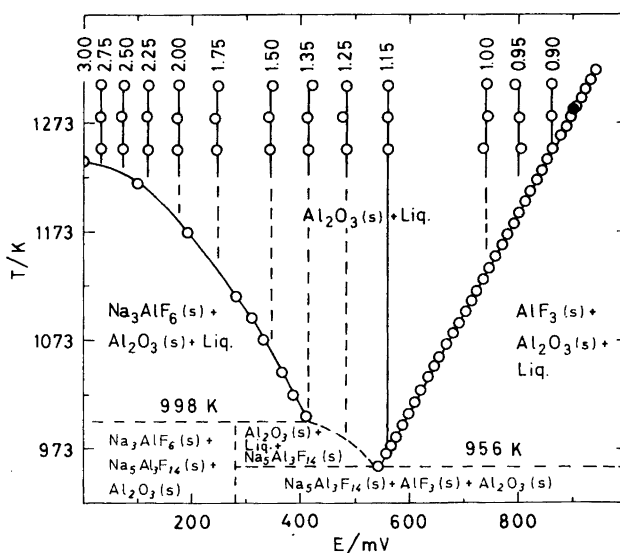

Fig. 3. The relationship between temperature and emf of cell [I] for various NaF − AlF₃ mol ratios as indicated on the top of each vertical line. Corresponding primary crystallization fields and univariant curves in the acidic part of the NaF − AlF₃ system saturated with alumina are given. ●, Emf of cell [I] obtained by using two aluminium electrodes.
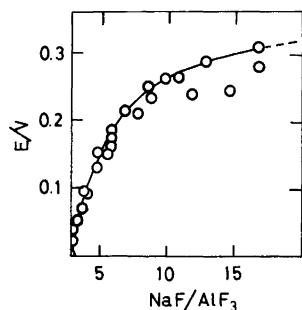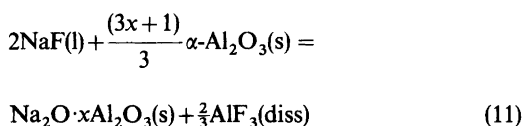
Fig. 4. The emf of cell [III] as a function of the mol ratio NaF$-$AlF$_3$ at 1278 K. The reference melt is Na$_3$AlF$_6$ saturated with alumina for which the emf is set equal to zero.

stable than the emf of the cells [I] and [II]. The cell voltage also decreased slightly with time. Such a drift in the cell voltage can be explained by the fact that the α-Al$_2$O$_3$ tube containing the oxygen electrode reacted gradually to β-Al$_2$O$_3$ (Na$_2$O·xAl$_2$O$_3$) according to the reaction scheme, eqn. (11).

$$2NaF(l)+\frac{(3x+1)}{3}\alpha\text{-Al}_2\text{O}_3(s)=$$

$$\text{Na}_2\text{O}\cdot x\text{Al}_2\text{O}_3(s)+\tfrac{2}{3}\text{AlF}_3(diss) \tag{11}$$

The numerical value of x is discussed below. This reaction reduced gradually the r-value of the melt and a drift in the emf must occur. Therefore, it seems reasonable to draw the curve in Fig. 4 in such a way that it fits the highest emf values obtained. Since it was difficult to obtain accurate emf data, no attempt was made to establish the relationship between cell voltage and temperature in basic melts.

Activity data. The emf of cell [I] can be expressed by the empirical eqns. (12) and (13).

$r<1.24$

$$E_1(V)=3.63 \ln\left(\frac{0.3}{r}+0.9\right)-0.3r+0.372 \tag{12}$$

$3>r>1.24$

$$E_1(V)=3.63 \ln\left(\frac{0.3}{r}+0.9\right) \tag{13}$$

The standard deviation is ±11.2 mV taking into account all experimental emf values. Using the average emf data shown in Fig. 3 the standard deviations is ±4.3 mV. An error of this magnitude corresponds to a very small compositional uncertainty as can be deduced from Fig. 3. When deriving the activity data, the emf of cell [II] shown in Fig. 2 was neglected since the values involved are low and less than the standard deviation of E_1.

It turns out that the emf of cell [III] can be described by an expression identical to eqn. (13), *i.e.* eqn. (14).

$r>3$

$$E_3(V)=3.63 \ln\left(\frac{0.3}{r}+0.9\right) \tag{14}$$

The curve in Fig. 4 is in fact drawn in agreement with eqn. (14). Since E_1 does not change with temperature it is in a first approximation assumed that E_3 also is independent of the temperature. This point is further discussed below.

Derivation of eqns. (12), (13) and (14) and combination with eqns. (5) and (6) followed by integration give empirical eqns. (15)$-$(18) for the natural logarithm of the activities, where r^* is the NaF/AlF$_3$ mol ratio of a melt saturated with both AlF$_3$ and Al$_2$O$_3$. The relationship between r^* and temperature is derived in eqn. (20). The last term in eqn. (16) is the natural logarithm of the activity at $r=1.24$ to be computed from eqn. (15) for the temperature in question.

$r^*<r<1.24$

$$\ln a_{\text{AlF}_3}=\frac{F}{RT}\left[1.361 \ln \frac{(3+r)(0.3+0.9r^*)}{(3+r^*)(0.3+0.9r)}+0.9r^*-0.9r+2.7 \ln \frac{(3+r)}{(3+r^*)}\right] \tag{15}$$

$1.24<r<15$

$$\ln a_{\text{AlF}_3}=\frac{F}{RT}\left[1.361 \ln \frac{(3+r)}{(0.3+0.9r)}-1.493\right]+\ln a_{\text{AlF}_3} \quad (r=1.24) \tag{16}$$

$15 > r > 1.24$

$$\ln a_{\text{NaF}} = \frac{F}{RT}\left[3.63 \ln r + 0.454 \ln (3+r) - 4.084 \ln (0.3+0.9r) - 0.423 \right] - 0.106 \qquad (17)$$

$1.24 > r > r^*$

$$\ln a_{\text{NaF}} = \frac{F}{RT}\left[3.63 \ln r + 1.354 \ln (3+r) - 4.084 \ln (0.3+0.9r) - 1.724 \right] - 0.106 \qquad (18)$$

These equations are valuable in conjunction with computer calculations and have been applied in connection with the development of an ionic structure model for cryolitic melts containing alumina.[12]

The temperature dependence of the emf of cell [I] corresponding to melts saturated with both AlF$_3$ and Al$_2$O$_3$ shown in Fig. 3 is well described by the empirical eqn. (19). The standard deviation is ± 4 mV. Combining eqns. (12) and (19) gives eqn. (20), which represents the relationship between temperature and composition of melts in equilibrium with solid AlF$_3$ and solid Al$_2$O$_3$. The numerical value of r^* for a given temperature can be estimated from Fig. 3 and determined more accurately from eqn. (20) by trial and error.

$$E_1(\text{V}) = 1.106 \times 10^{-3}T - 0.514 \qquad (19)$$

$$T(\text{K}) = 3282 \ln \left[\frac{0.3}{r^*} + 0.9 \right] - 271.2 r^* + 801 \qquad (20)$$

Activity data for NaF have also been fitted to equations of the type (21). Table 1 shows the results.

Table 1. Calculated values for A in the equation, $\ln a_{\text{NaF}} = (A/T) - 0.106$, where $\ln a_{\text{NaF}}$ is the natural logarithm of the activity of NaF in NaF$-$AlF$_3$ melts saturated with alumina at $T < 1300$ K. The standard state is liquid NaF, while the composition given by the mol ratio NaF$-$AlF$_3$ is denoted r.

r	A	r	A	r	A
0.90	-8000	2.20	-2080	3.70	-880
1.00	-6860	2.40	-1810	4.9	-770
1.20	-5040	2.60	-1600	5.0	-500
1.40	-4010	2.80	-1410	6.0	-350
1.60	-3330	3.00	-1260	8.0	-180
1.80	-2810	3.20	-1130	10	-90
2.00	-2400	3.40	-1020	15	0

$$\ln a_{\text{NaF}} = A/T + B \qquad (21)$$

The temperature dependence of the activity of AlF$_3$ cannot be described by such a simple equation as eqn. (21). Therefore, some activity data for AlF$_3$ at two different temperatures are shown in Table 2.

A comparison of activity data from various sources is made in Table 3. Yoshida and Dewing[3] derived activity data from the emf of cell [I] with two aluminium electrodes and from the sodium content of aluminium assumed to be in equilibrium with the melt. Kvande[13] estimated the activity data shown in

Table 2. The natural logarithm of the activity of AlF$_3$ in NaF$-$AlF$_3$ melts saturated with alumina ($-\ln a$). The NaF$-$AlF$_3$ mol ratio is denoted r. The standard state is solid AlF$_3$.

r	1237 K	1300 K	r	1237 K	1300 K
0.90	0.000	0.367	2.80	7.532	7.591
1.00	0.816	1.200	3.00	7.890	7.931
1.20	2.430	2.736	3.20	8.215	8.240
1.40	3.500	3.753	3.70	8.915	8.906
1.60	4.326	4.540	4.0	9.272	9.246
1.80	5.040	5.219	5.0	10.218	10.146
2.00	5.663	5.812	6.0	10.909	10.803
2.20	6.212	6.335	8.0	11.851	11.699
2.40	6.701	6.800	10.0	12.465	12.283
2.60	7.138	7.216	15.0	13.346	13.127

Table 3. Activity data of NaF and AlF$_3$ in Na$_3$AlF$_6$ melts saturated with α-Al$_2$O$_3$. The standard states are liquid NaF and solid AlF$_3$.

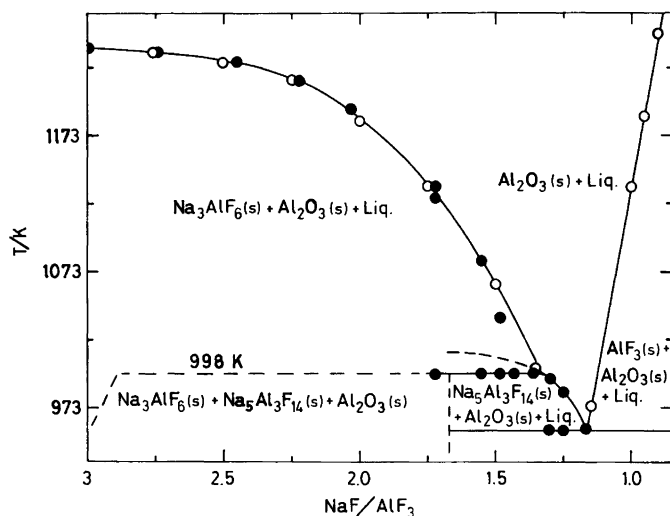| Authors	T/K	a_{NaF}	a_{AlF_3}
Yoshida and Dewing[3]	1273	0.31	5.8×10^{-4}
Kvande[13]	1300	0.30	5×10^{-4}
This work	1273	0.334	3.64×10^{-4}
This work	1300	0.341	3.60×10^{-4}

Fig. 5. Primary crystallization fields in the acidic part of the NaF $-$ AlF$_3$ system saturated with alumina. NaF $-$ AlF$_3$ denotes the mol ratio. ● Cryoscopic data. ○, Emf $-$ temperature $-$ composition points from the data given in Fig. 3.

Table 3 from the total vapour pressure and the average molar mass of the vapour. The discrepancies between the literature values and the present data cannot be explained exclusively by the experimental uncertainties in the emf values of the present work. It should be emphasized that the variations of the activities with temperature and composition in acidic melts are quite well described by the present data. The accuracy of the data in the basic range is discussed below.

Phase diagram data. The constant emf values corresponding to the given melt compositions shown in Fig. 3 are extrapolated linearly (dashed lines) to the univariant curves. Melt compositions

and temperatures corresponding to these univariant curves are replotted in Fig. 5 together with phase diagram data obtained from cryoscopic measurements. As may be seen from the figure the two sets of data are in very good agreement, which means that the emf values given in Fig. 3 are fairly accurate. The previous assumption that the emf of cell [I] is independent of temperature is justified for a given melt composition in the acidic range.

Ternary eutectic and peritectic data from various sources [7,14–17] are given in Table 4. The composition of the ternary eutectic point represented by the r-value, seems to be well defined. The eutectic and peritectic temperatures de-

Table 4. Ternary eutectic and peritectic data for the system Na$_3$AlF$_6$ $-$ AlF$_3$ $-$ Al$_2$O$_3$. The NaF $-$ AlF$_3$ mol ratio is denoted r.

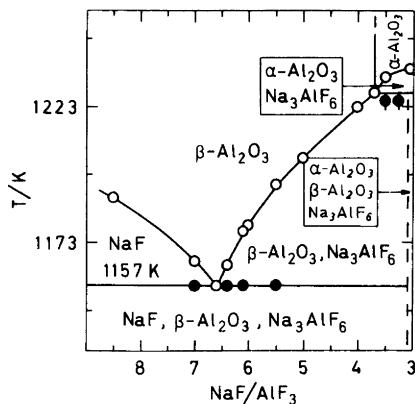| Authors	Ref.	Eutectic data		Peritectic data	
		T/K	r	T/K	r
Philips *et al.*	7	938	1.16		1.44
Fuseya *et al.*	14	938	1.16	980	1.46
Fenerty *et al.*	15				1.44
Rolin	16	945	1.18	983	1.43
Foster	17	957	1.17	996	1.45
Present work		956	1.17	998	1.33
		±2	±.01	±2	±.02

Fig. 6. Cryoscopic data in the basic part of the NaF −AlF$_3$ system saturated with either α-Al$_2$O$_3$ or β-Al$_2$O$_3$. The liquid phase present above the solidus (1157 K) is not denoted on the figure. NaF − AlF$_3$ indicates the mol ratio.

termined by Fuseya *et al.*[14] and Rolin[16] are obviously too low presumably due to supercooling. The peritectic melt composition resulting from the present work corresponding to $r = 1.33 \pm 0.02$, differs considerably from the literature data given in Table 4. In the present work it was not possible to obtain reliable liquidus temperatures by cryoscopy in the range $1.50 > r > 1.33$. However, a well-defined and constant solidus temperature of 998 ± 2 K was established in this range, which means that the peritectic composition $r = 1.33$ cannot be much in error.

Fig. 6 shows stability fields close to the cryolite corner of the Na$_3$AlF$_6$ − NaF − Al$_2$O$_3$ system. The cryoscopic data in the range $3 < r < 4$ were determined for melt compositions containing 12 wt % Al$_2$O$_3$. This concentration is only slightly higher than the saturation limit corresponding to the univariant line. The eutectic temperature in the binary system Na$_3$AlF$_6$ − Al$_2$O$_3$ was found to be 1237 ± 1 K which is in agreement with or slightly higher than most of the literature data cited by Grjotheim *et al.*[1]

The peritectic point where the solid phases α-Al$_2$O$_3$, β-Al$_2$O$_3$ and β-Na$_3$AlF$_6$ coexist in equilibrium with the melt is located at $r = 3.7 \pm 0.1$ and at 1228 ± 2 K. The peritectic reaction is given in eqn. (22). For melt compositions in the range

$$12NaF(l) + (3x + 1)\alpha\text{-}Al_2O_3(s) =$$
$$3Na_2O \cdot xAl_2O_3(s) + 2Na_3AlF_6(s) \quad (22)$$
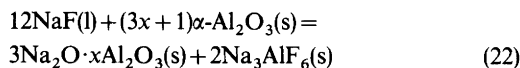
$3.0 < r < 3.7$ and alumina concentrations corresponding to the univariant curve, α-Al$_2$O$_3$ and β-Na$_3$AlF$_6$ will precipitate until the peritectic point is reached. At the peritectic temperature reaction (22) proceeds to the complete consumption of either the melt (NaF) or of solid α-Al$_2$O$_3$.

By use of reaction (22) and an alumina (Al$_2$O$_3$) solubility of 18 mol per cent it is calculated that the final compounds of crystallization are α-Al$_2$O$_3$, β-Al$_2$O$_3$* and Na$_3$AlF$_6$ for melt compositions in the range $3.00 < r < 3.10$. It should be emphasized that the upper limit of the range depends on the amount of alumina present initially. The final products of crystallization in the neighbouring field are NaF, Na$_3$AlF$_6$ and β-Al$_2$O$_3$ as indicated in Fig. 6.

Foster[18] found that the boundary line separating the primary crystallization field of α-Al$_2$O$_3$ and β-Al$_2$O$_3$ varied slightly with the NaF content of the melt in the temperature range 1229 − 1330 K. The location of the peritectic point was found to be r = 3.40 at 1229 K, a temperature in agreement with the present study. The melt composition given by Foster for the peritectic point is then slightly different from $r = 3.7 \pm 0.1$ found in the present work. However, taking the average composition data defining the α-Al$_2$O$_3$, β-Al$_2$O$_3$ univariant line in the range 1229 − 1330 K from the work of Foster,[18] one finds $r = 3.7 \pm 0.3$ in agreement with the present study. It is believed that this interpretation of the data is correct. The line is indicated in Figs. 1 and 6.

The ternary eutectic point shown in Fig. 6 located at $r = 6.6 \pm 0.1$ and $T = 1157 \pm 2$ K is in fair agreement with data given by Foster[18] and Holm.[19]

Activities of liquid NaF are calculated at temperatures corresponding to the points defining the NaF/β-Al$_2$O$_3$ univariant curve shown in Fig. 6. The calculations are based on standard Gibbs energies from the JANAF tables[21] for reaction (23)

$$NaF(s) = NaF(l) \quad (23)$$

and the assumption of no solid solubility. The activities calculated in this way are compared with corresponding data from the present work as shown in Table 5. The maximum deviation between these

---

*If the stoichiometric formula is taken to be Na$_2$O·9Al$_2$O$_3$ the range will be $3.00 < r < 3.10$. If the formula is taken to be Na$_2$O·11Al$_2$O$_3$ the range will be $3.00 < r < 3.08$. In these calculations the system is taken to be constituted of the compounds NaF, Na$_3$AlF$_6$ and Al$_2$O$_3$.

Table 5. Comparison of activities of liquid NaF at various temperatures and melt compositions expressed by the mol ratio NaF−AlF₃ denoted r.

T/K	r	a_{NaF}[a]	a_{NaF}[b]
1157	6.60	0.736	0.706
1166	7.00	0.755	0.729
1189	8.50	0.809	0.793

[a] From JANAF tables. [b] Present work.

two sets of data is at the ternary eutectic point and amounts to 4.2 %.

The activities obtained using the JANAF data will be lowered and brought into better agreement with the present data if some solid solubility is assumed in the stability field of solid NaF. However, it is possible that there is a minor error in the temperature dependence of the activities in the basic range of the present work. Nevertheless, the results given in Table 5 show that eqns. (16) and (17) can be used to calculate activities as a function of temperature with reasonable accuracy also in basic melts. It is believed that the error in the present activity data will not exceed 5 % of the absolute values given in eqns. (15)−(18) for melts saturated with alumina and for $T < 1300$ K.

Thermodynamic data for formation of β-Al₂O₃. The value of x in Na₂O·xAl₂O₃ (β-Al₂O₃) coexisting with α-Al₂O₃ is not accuractely known.[20] It is, however, generally accepted that the numerical value is in the range $9 \leq x \leq 11$. The corresponding equilibrium is conveniently expressed by reaction (11). The standard Gibbs energy change of this reaction is then calculated from the present activity data for $r = 3.7$, keeping in mind that the activities of α-Al₂O₃ and β-Al₂O₃ are equal to unity. The results are tabulated for various temperatures in Table 6 together with standard enthalpy and entropy data for the reaction. The enthalpy data given are derived from the slope obtained by plotting $\Delta G^\circ/T$ versus $1/T$. The data given in Table 6 combined with standard thermodynamic data for NaF(l),[21]

Table 6. Standard thermodynamic properties of the reaction $2\,NaF(l) + \frac{(3x+1)}{3}\,\alpha\text{-Al}_2O_3(s) = Na_2O \cdot xAl_2O_3(s) + \frac{3}{3}AlF_3(s)$.

T/K	$\Delta G^\circ/kJ$	$\Delta H^\circ/kJ$	$\Delta S^\circ/(J/degree)$
1180	41.539[a]		
1200	42.526[a]	−16.300	−49.022
1220	43.522[a]		
1228	43.873		
1240	44.468		
1260	45.426		
1280	46.334		
1300	47.250	−11.460	−45.162
1320	48.175[a]		
1350	49.480[a]		
1400	51.643[a]	−7.690	−42.381
1500	55.798[a]		

[a] Extrapolated values.

AlF₃(s)[21] and α-Al₂O₃(s)[22] give the standard formation properties of Na₂O·xAl₂O₃ shown in Table 7. The uncertainty in the Gibbs energies is estimated to be ±x kJ. The only other thermodynamic data for β-Al₂O₃ known to the authors are from a work of Weber described by Kummer,[20] for a solid state electrolyte cell reaction proposed to be as given in eqn. (24).

$$2NaAlO_2(s) + (x-1)\,\alpha\text{-Al}_2O_3(s) = Na_2O \cdot xAl_2O_3(s) \quad (24)$$
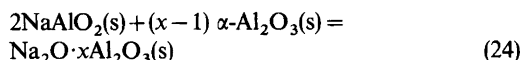
Thermodynamic properties of this reaction calculated from the emf values of Weber and shown in Table 8 do not compare favourably with corresponding data from the present work for β-Al₂O₃ (Table 7) and data for NaAlO₂(s)[21] and α-Al₂O₃(s)[22] from the JANAF tables. For a solid state reaction of the type described by reaction (24) the entropy change is expected to be rather small. The data for β-Al₂O₃ resulting from the present work are in agreement with this principle while those derived by Weber from emf measurements are not.

Table 7. Standard formation data of Na₂O·xAl₂O₃ (β-Al₂O₃) in equilibrium with α-Al₂O₃.

T/K	ΔG_f° kJ/mol	ΔH_f° kJ/mol	ΔS_f° (J/mol, degree)
1200	−1295.103x−485.100	−1691.662x−844.950	−330.466x−299.875
1300	−1262.099x−455.512	−1690.482x−834.608	−329.525x−291.612
1400	−1229.188x−426.689	−1689.215x−825.532	−328.591x−284.888

Table 8. Thermodynamic data calculated from the emf values of Weber described by Kummer[20] for the reaction $2NaAlO_2(s)+(x-1)$ α-$Al_2O_3(s) =$ $Na_2O \cdot xAl_2O_3(s)$ and corresponding data from the present work (β-Al_2O_3) and from the JANAF tables ($NaAlO_2$,[21] α-Al_2O_3 [22]).

T/K	$\Delta G°/kJ$	$\Delta H°/kJ$	$\Delta S°/(J/degree)$
1200	-34.340	17.260	43.0
1300	-38.640	17.260	43.0
1400	-42.940	17.260	43.0
1200^a	-48.346	-59.994	-9.707
1300^a	-47.643	-52.631	-3.837
1400^a	-47.472	-46.739	0.523

^{a} From JANAF tables.

Without discussing details it should be emphasized that the overall cell reaction (24) proposed by Kummer[20] is not completely correct, which means that some deviations from the present data are to be expected.

Another set of interesting data are obtained when properties for solid and liquid NaF from the JANAF tables[21] are combined with data in Table 6 for reaction (11). The results for the solid state reaction given in Table 9 show reasonable values for the entropy change.

The stability of β-Al_2O_3 may be illustrated by reaction (25). The data given in Table 10 show that β-

$$Na_2O(s) + x\alpha\text{-}Al_2O_3(s) = Na_2O \cdot xAl_2O_3(s) \qquad (25)$$
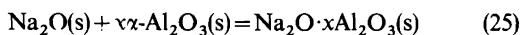
Al_2O_3 is a fairly stable compound. As expected the entropy change of the reaction turns out to be small.

Thermodynamic data for solid Na_3AlF_6. The standard Gibbs energy change associated with

Table 9. Thermodynamic properties of the solid state reaction $2NaF(s) + \dfrac{(3x+1)}{3}$ α-$Al_2O_3(s) =$ $Na_2O \cdot xAl_2O_3(s) + \frac{2}{3}AlF_3(s)$. Data is from the present work (Table 6) and from the JANAF tables for NaF.

T/K	$\Delta G°/kJ$	$\Delta H°/kJ$	$\Delta S°/(J/degree)$
1200	46.133	49.647	2.929
1300	45.618	55.413	7.535
1400	44.723	59.446	10.517

Table 10. Thermodynamic properties of the reaction $Na_2O(s) + x\alpha\text{-}Al_2O_3(s) = Na_2O \cdot xAl_2O_3(s)$. Data for β-Al_2O_3 are from the present work (Table 7) while data for α-Al_2O_3 and Na_2O are from the JANAF tables.[22,21]

T/K	$\Delta G°/kJ$	$\Delta H°/kJ$	$\Delta S°/(J/degree)$
1200	-234.764	-240.153	-4.489
1300	-234.019	-245.567	-8.883
1400	-233.317	-240.463	-5.104

$$3NaF(l) + AlF_3(s) = Na_3AlF_6(s) \qquad (26)$$

$$\Delta G°(26) = RT \ln a_{NaF}^3 a_{AlF_3} \qquad (27)$$

reaction (26) can be expressed by eqn. (27) if Na_3AlF_6 is in its standard state. For melt compositions along the univariant line shown in Fig. 5, the requirement of unit activity of Na_3AlF_6 is fulfilled in the temperature range $998\ K < T < 1237$ K provided that there is no solid solubility. The Gibbs energy is then readily calculated from the activity data described above. It should be remembered that the standard states of the activities are liquid NaF and solid AlF_3. Fig. 7 shows the results of the calculations. Three points calculated from the work of Dewing,[23] obtained with solid state electrochemical cells, have been included after appropriate adjustment of standard states. These points, which are outside the temperature range of the present work, seem to give a nice overall fit. The data shown in Fig. 7 with the exception of those derived from basic melts, are fitted to a straight line,
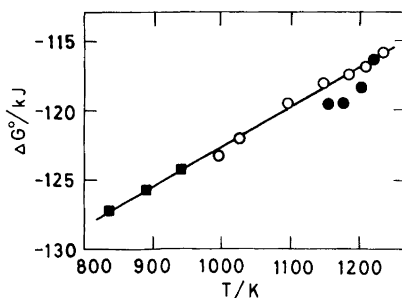

Fig. 7. The standard Gibbs energy of the reaction $3NaF(1) + AlF_3(s) = Na_3AlF_6(s)$ as a function of temperature. ■, From the work of Dewing.[23] ○, ●, Present data corresponding to the univariant curves on the acidic and the basic side of the cryolite composition, respectively.

eqn. (28). The standard deviation in the Gibbs energy is ± 0.25 kJ.

$$\Delta G°(26) = -151.745(\pm 0.550) + 0.0290(\pm 0.0005)T \text{ (kJ)} \tag{28}$$

The derivation of the activity data in the basic range ($r > 3$) was based on the assumption of a temperature independent emf of cell [III], eqn. (14). The activity data derived and based on this assumption are used to determine the variation in the Gibbs energy of reaction (26) for temperatures and melt compositions defining the univariant curve in Fig. 6, where solid Na$_3$AlF$_6$ is in equilibrium with the melt. As shown in Fig. 7 these data deviate slightly from the corresponding values obtained on the acidic side of the cryolite composition. However, the deviation is small and within the experimental uncertainty of the activity data discussed above.

From a study of the cryolite liquidus curve of the binary NaF − AlF$_3$ system and from electrical resistivity measurements, Dewing[24,25] concluded that cryolite is a non-stoichiometric compound containing AlF$_3$ in solid solution at temperatures above 838 K. The present data do not directly support this hypothesis, although a minor solid solubility within the limits of experimental uncertainty is to be expected.

The free energy function $(\Delta G° - \Delta H°_{298})/T$ of reaction (26) can be calculated for any temperature by linear interpolation of the data in the JANAF tables.[21] $\Delta H°_{298}$ is then calculated for all the $\Delta G°$ and T values obtained on the acidic side of the system and shown in Fig. 7. Corresponding $\Delta H°_{298}$ and T values are plotted in Fig. 8. The apparent variation of $H°_{298}$ with temperature can hardly be explained only by errors in the present activity data. This

Table 11. Standard Gibbs energy of formation of solid Na$_3$AlF$_6$. The differences between $\Delta G°$ from the present work and from the JANAF tables[21] are denoted $\Delta(\Delta G°)$.

T/K	$\Delta G°_f$/kJ	$\Delta(\Delta G°_f)$/kJ
800	−2871.333[a]	−6.360
900	−2818.715	−7.117
1000	−2766.101	−7.661
1100	−2714.060	−8.619
1200	−2657.032	−9.820
1300	−2581.766[a]	−10.770

[a] Extrapolated values.

means that the free energy function of reaction (26) from the JANAF tables[21] is not strictly correct and a minor revision is needed. The shape of the curve in Fig. 8 may indicate that a constant value for $\Delta H°_{298}$ is approached with decreasing temperature. It is believed that the major part of the discrepancy can be related to the data for solid Na$_3$AlF$_6$ given in the JANAF tables.[21]

The standard Gibbs energy of formation of solid Na$_3$AlF$_6$ is calculated from eqns. (26) and (28) and Gibbs energy data for NaF(l) and AlF$_3$(s) from the JANAF tables.[21] The values are shown in Table 11 together with the difference in $\Delta G°$ resulting from the present work and from the JANAF tables.[21] The discrepancies between the two sets of data decrease rapidly with decreasing temperature.

Thermodynamic data for solid Na$_5$Al$_3$F$_{14}$. The standard Gibbs energy change of reaction (29) was determined from the present activity data and the points defining the univariant curve shown in Fig. 5
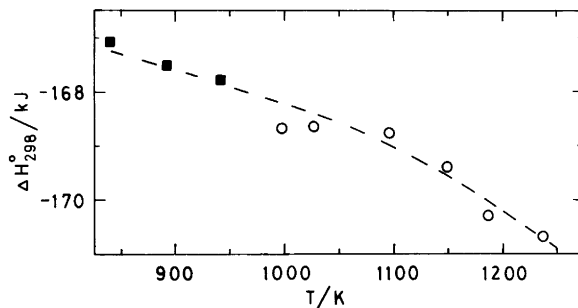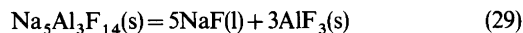
$$Na_5Al_3F_{14}(s) = 5NaF(l) + 3AlF_3(s) \tag{29}$$

Fig. 8. Apparent temperature variation of $\Delta H°_{298}$ for the reaction 3NaF(l) + AlF$_3$(s) = Na$_3$AlF$_6$(s). ■, Calculated from the work of Dewing.[23] ○, Present work.

Table 12. Standard Gibbs energy change of the reaction $Na_5Al_3F_{14}(s) = 5NaF(l) + 3AlF_3(s)$.

T/K	$\Delta G°/kJ$	T/K	$\Delta G°/kJ$
998	223.421	985	223.480
994	223.505	956	223.714

where solid chiolite $(Na_5Al_3F_{14})$ is in equilibrium with the melt. The results are shown in Table 12. A second-law treatment of the data gives eqn. (30). The

$$\Delta G°(29) = 229.890 - 0.00647T \text{ (kJ)} \tag{30}$$

standard errors in the enthalpy and entropy terms are ± 1.29 kJ and ± 0.00013 kJ/degree, respectively. The standard deviation of $\Delta G°$ is ± 0.043 kJ. The real uncertainties are considerably larger than these statistical values, since there may be some solid solubility of AlF_3 in chiolite.[25] It should be recalled that the standard states of the activities are liquid NaF, solid AlF_3 and solid $Na_5Al_3F_{14}$.

Eqn. (30) combined with thermodynamic data for $NaF(l)$ and $AlF_3(s)$ gives the standard Gibbs energy of formation of chiolite, eqn. (31), strictly valid only in the range $956 < T < 998$ K.

$$\Delta G_f° = -7474.911 + 1.17919T(\text{kJ}) \tag{31}$$

Thermochemical data for solid $Na_5Al_3F_{14}$ obtained in the present study are compared with previously published values (partly updated) in Table 13. Grjotheim *et al.*[26] derived the standard Gibbs energy change of reaction (32) at temperatures around 900 K to be as given in eqn. (33).

$$5/3 \, Na_3AlF_6(s) + 4/3 \, AlF_3(s) = Na_5Al_3F_{14}(s) \tag{32}$$
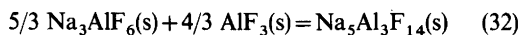
$$\Delta G° = 12.55 - 0.0251T \text{ (kT)} \tag{33}$$

Thermodynamic data for solid $Na_5Al_3F_{14}$ are then derived from these equations using data for solid Na_3AlF_6 from the present work, while data for liquid NaF and solid AlF_3 are from the JANAF tables.[21] The results are given in Table 13. Cantor *et al.*[27] studied the equilibrium vapour pressure of $BF_3(g)$ according to reaction (34). Cantor *et al.*[27]

$$4/3 \, NaBF_4(l) + 1/3 \, Na_5Al_3F_{14}(s) =$$
$$Na_3AlF_6(s) + 4/3 \, BF_3(g) \tag{34}$$
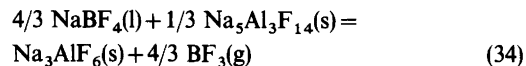
used the standard Gibbs energy of solid Na_3AlF_6 from the work of Dewing,[23] shown to be in excellent agreement with the present data, when deriving the thermodynamical data for chiolite shown in Table 13. The results of Dewing included in the table are based on emf measurements of solid electrolyte galvanic cells corresponding to reaction (35) and of

$$5NaF(s) + 3AlF_3(s) = Na_5Al_3F_{14}(s) \tag{35}$$
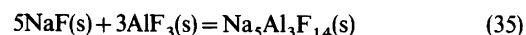
thermodynamic data for NaF(s) and $AlF_3(s)$ from the JANAF tables.[21]

The good agreement between the Gibbs energy data from the different sources shown in Table 13 should be noted.

Thermodynamic data for liquid $NaAlF_4$. The equilibrium constant of reaction (36) was derived to

$$NaF(l) + AlF_3(s) = NaAlF_4(l) \tag{36}$$
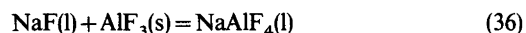
be 476 at 1285 K in a previous paper.[12] The derivation was based on the assumption of an ideal Temkin activity of $NaAlF_4$ and on liquid NaF and solid AlF_3 as standard states. It can be estimated that the ideal Temkin activity in a pure $NaAlF_4$ melt is 0.95 ± 0.05 at 1285 K. Defining the activity of pure $NaAlF_4(l)$ as equal to one results in an equilibrium constant of 476/0.95 at 1285 K.

The next step is to derive a reasonable value for

Table 13. Standard Gibbs energy, enthalpy and entropy of formation of solid $Na_5Al_3F_{14}$ at 900 K.

Source	$\Delta G_f°/kJ$	$\Delta H_f°/kJ$	$\Delta S_f°/(J/degree)$
Dewing[23]	-6423.322	-7539.878	-1240.62
Grjotheim *et al.*[26]	-6408.908	-7472.984	-1182.306
Cantor *et al.*[27]	-6425.118	-7488.523	-1181.562
This work[a]	-6413.618	-7462.515	-1165.441

[a] Extrapolated from eqn. (30) and combined with data from the JANAF tables.

the equilibrium constant for eqn. (36) from activities corresponding to the ternary eutectic point $r = 1.17$ and $T = 956$ K. The activity of AlF$_3$ is unity, while that of NaF is found from eqn. (18) to be 3.59×10^{-3}. The activity of NaAlF$_4$ must be estimated. In a pure NaF–AlF$_3$ melt with $r = 1.17$ the anion fraction of AlF$_4^-$ is approximately 0.85. Adding the relatively small amount of Al$_2$O$_3$ needed to reach the ternary eutectic point [17] the anion fraction of AlF$_4^-$ is reduced to 0.70–0.75. The thermodynamic activity of NaAlF$_4$ corresponding to the ternary eutectic is then expected to be 0.75 ± 0.10. A second-law calculation then gives eqn. (37) for the standard

$$\Delta G^\circ(36) = 27.167 - 0.07283T \text{ (kJ)} \tag{37}$$

Gibbs energy change of reaction (36). The standard Gibbs energy of formation of NaAlF$_4$ is then derived by use of data for NaF(l) and AlF$_3$(s) from the JANAF tables,[21] eqn. (38). The entropy of formation

$$\Delta G_f^\circ, \text{NaAlF}_4(\text{l}) = -2024.930 + 0.2648T \text{ (kJ)} \tag{38}$$

of NaAlCl$_4$(l) in the corresponding chloride system was recently derived [28] to be -0.2639 kJ/(mol,degree) which compares favourably with the entropy term in eqn. (38). From the data given, the activity of NaAlF$_4$ is readily calculated for whatever temperature and composition within the validity range of the activity data of NaF and AlF$_3$.

Transport numbers. It is assumed that the only uncomplexed ions, Na$^+$ and F$^-$, are responsible for the transport of all current in the system. In order to assess the variation of the transport numbers with composition, the emf of cell [II] is conveniently

$$E_2(\text{V}) = 0.019a_{\text{NaF}}^2 - 0.0021 \tag{39}$$

$$dE_2 = 0.038a_{\text{NaF}}da_{\text{NaF}} \tag{40}$$

expressed by the empirical eqn. (39), which may be written as eqn. (40). The fit to the experimental data is satisfactory as illustrated by the straight line in Fig. 9.

The differential form of the emf of cell [II], eqn. (41), combined with eqn. (40) gives eqn. (42) for the

$$dE_2 = \frac{RT}{F}(1\text{-}t_{\text{Na}} +)\text{d} \ln a_{\text{NaF}} \tag{41}$$

$$t_{\text{Na}} + = 1 - 0.038 \frac{F}{RT} a_{\text{NaF}}^2 \tag{42}$$

transport number of Na$^+$. The transport number plotted in Fig. 10 indicates clearly, as one may expect, that the current carried by F$^-$ $(1\text{-}t_{\text{Na}}+)$ is increasingly important as the basicity of the melt increases. The transport number of Na$^+$ derived agrees reasonably well with the results of Frank and Foster [29] who investigated transport phenomena in the Na$_3$AlF$_6$–Al$_2$O$_3$ system by means of radioactive tracers. The present data are also in general agreement with the work reported by Tual and Rolin.[30] These authors found the transference number of Na$^+$ to be slightly less than unity and that F$^-$ carried the rest of the current.

It should be emphasized that eqn. (42) is strictly valid only in the range $2 < r < 3$. However, extrapolation outside this range gives reasonable results. For pure NaF at 1285 K eqn. (42) gives $t_{\text{Na}} + = 0.66$ in agreement with $t_{\text{Na}} + = 0.64 \pm 0.05$ determined experimentally by Grjotheim *et al.*[31]
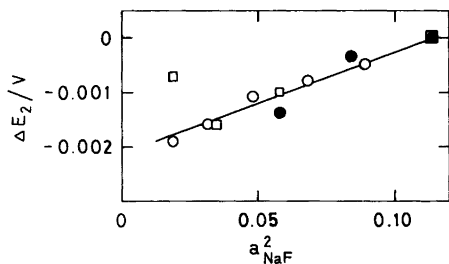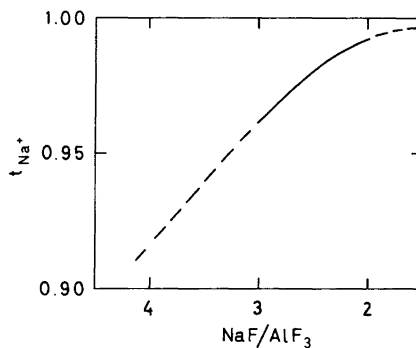

Fig. 9. The emf of cell [II] as a function of the square of the sodium fluoride activity in NaF–AlF$_3$ melts saturated with alumina at 1278 K. One symbol for each series of experiments.

Fig. 10. The transport number of Na$^+$ as a function of the NaF–AlF$_3$ mol ratio in NaF–AlF$_3$ melts saturated with alumina at 1278 K.
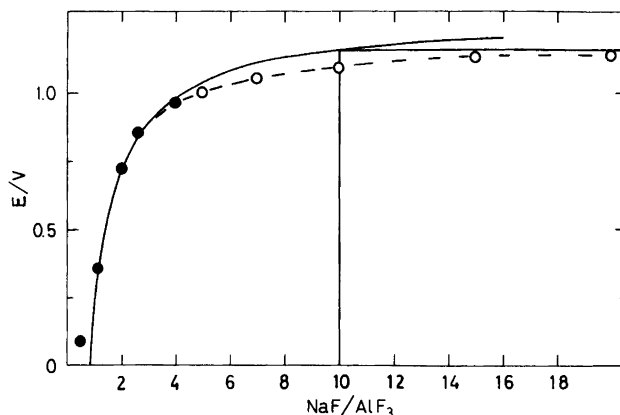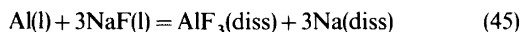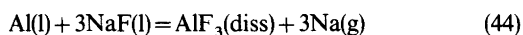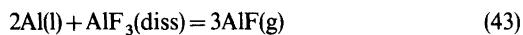
Fig. 11. Emf as a function of the $NaF - AlF_3$ mol ratio in melts saturated with alumina. The fully drawn curve corresponds to eqns. (12) — (14) while ● and ○ are data points replotted from Yoshida and Dewing [3] and Thonstad and Rolseth,[4] respectively (see text). Temperature: 1273 to 1295 K.

The activity data in the acidic range ($r < 3$) was derived by setting E_2 equal to zero. The error introduced by doing this can be shown to be only of minor importance.

The $NaF - AlF_3 - Al_2O_3$ *system in presence of liquid aluminium.* The emf expressed by eqns. (12) — (14) is shown in Fig. 11 (fully drawn line) together with corresponding data of a cell with two aluminium electrodes [3,4,32] (broken line). The present work revealed that the emf of the cell with aluminium electrodes was in agreement with that of the corresponding cell using oxygen electrodes in the acidic range of the system. Thus, it is convenient to choose a melt saturated with AlF_3 and Al_2O_3 as the reference for the emf as indicated in Fig. 11. The present data for acidic melts agree quite well with the data of Yoshida *et al.*[3] except for their data concerning the reference melt which obviously are in error.

As shown in Fig. 11 there is an increasing discrepancy in the two sets of data with increasing basicity. Only a minor part of this discrepancy can be explained by the fact that the transport number of Na^+ decreases with increasing NaF content of the melt. The possible contribution of electronic conductivity is believed to be of minor importance. A rational discussion of the discrepancies between the two sets of emf data shown in Fig. 11 should be based on the equilibria (43) — (45). The apparent

$$2Al(l) + AlF_3(diss) = 3AlF(g) \qquad (43)$$

$$Al(l) + 3NaF(l) = AlF_3(diss) + 3Na(g) \qquad (44)$$

$$Al(l) + 3NaF(l) = AlF_3(diss) + 3Na(diss) \qquad (45)$$

equilibrium vapor pressures of AlF(g) and Na(g) as a function of the composition are shown in Fig. 12. The vapour pressures on the acidic side of the system are so small that they do not effect the emf to any extent. However, on the basic side the vapour pressure of sodium reaches one atmosphere at $r = 10$. The emf corresponding to this composition is shown as a straight horizontal line in Fig. 11. If the
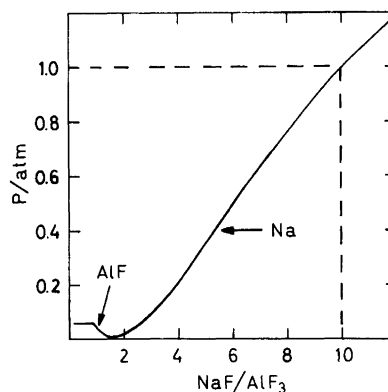

Fig. 12. Apparent equilibrium vapour pressures of Na(g) and AlF(g) as a function of the mol ratio NaF $- AlF_3$ in NaF $- AlF_3$ melts saturated with alumina at 1285 K. The calculations are based on equilibrium constants for eqns. (43) and (44) obtained from the JANAF tables [21] and activity data from the present work.

concentration cell with aluminium electrodes constitutes an open system one will expect the cell potential to approach this horizontal line in Fig. 11 as the basicity of the melt increases. The results shown indicate clearly that the melt in contact with the aluminium surface approaches the composition $r = 10$ at increasingly high NaF content of the melt. This means that there is a steady state equilibrium on the metal $-$ melt interface [eqn. (45)], with compositional variations in the adjacent diffusion layer on the electrolytic side of the interface. When the vapour pressure of sodium is less than one atmosphere at the interface the relationship (46)

$$J_{NaF} = -3J_{AlF_3} = -J_{Na(diss)} \qquad (46)$$

between the mass fluxes may be valid. From the results given in Fig. 11 and eqn. (46) one expects these fluxes and the corresponding concentration gradients to become increasingly important with increasing basicity if the experimental set-up corresponds to an open system. It follows that the equilibrium concentration of dissolved metal [Na(diss)] must be relatively high in basic melts.

A rough estimate of the metal solubility of a melt with an original composition of $r = 10$ from the work of Thonstad,[33] yields a value of 0.6 when the solubility is expressed as weight per cent aluminium. It is readily calculated that an original r-value of 10 will be lowered to 8.6, if the metal solubility reaction is correctly described by eqn. (45). In an open system the immediate lowering of the r-value in the bulk of the melt is not so large, since the bulk phase is not in equilibrium with the aluminium metal. In this case, however, a gradual decrease in the r-value of the bulk phase must occur, even to values below 8.6, since sodium continuously escapes to the surroundings.

In a previous work[2] it was found that the cell [IV] should be decribed by the emf eqn. (47), where

Al|Na$_3$AlF$_6$(l), Al$_2$O$_3$(s)||Na$_3$AlF$_6$(l),

Al$_2$O$_3$(s)|(Pt), O$_2$ (1 atm)   [IV]
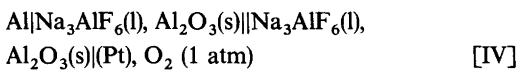
$$E_{IV} = E^{\circ}_{Al_2O_3} - \frac{RT}{F} \ln \frac{a_{NaF}}{a_{NaF(I)}} +$$

$$\frac{RT}{3F} \ln \frac{a_{AlF_3}}{a_{AlF_{3(I)}}} \qquad (47)$$

$E^{\circ}_{Al_2O_3}$ is the standard emf for the formation of α-Al$_2$O$_3$ and (I) denotes activities in the left-hand side

compartment. The experimental results[2] showed that the activities of NaF and AlF$_3$ in the left-hand side compartment were not equal to those in the other compartment, in spite of the fact that the original compositions were identical. The activity terms of eqn. (47) corresponded to approximately 12 mV which is equivalent to a shift in the melt composition from $r = 3.00$ to $r = 2.90$. A metal solubility of 0.10 weight % aluminium[1,33] combined with eqn. (45) gives an apparent change in the r-value from 3.00 to 2.95. Thus, the metal solubility reaction explains, at least partly, the observed change in the r-value. However, also in this case it is suggested that the main reason for the change of the r-value can be related to concentration gradients in the diffusion layer on the electrolytic side of the metal $-$ melt interface. This interpretation means that an aluminium electrode in the basic part of an open system behaves reversibly as regards the melt on its surface, but not with respect to the bulk properties. Another important conclusion to be drawn is that the metal dissolution reaction in basic melts should be studied in a closed system, where sodium is not allowed to escape to the surroundings. This conclusion is supported by a recent study of Rolseth[34,35] concerning the reoxidation reaction in aluminium electrolysis.

REFERENCES

1. Grjotheim, K., Krohn, C., Malinovsky, M., Matiasovsky, K. and Thonstad, J. *Aluminium Electrolysis*, Aluminium Verlag, Düsseldorf 1977.
2. Sterten, Å., Haugen, S. and Hamberg, K. *Electrochim. Acta 21* (1976) 589.
3. Yoshida, K. and Dewing, E. W. *Met. Trans. 3* (1972) 683.
4. Thonstad, J. and Rolseth, S. *Proc. ICSOBA 3rd Int. Meeting*, Nice 1973, 657.
5. Ratkje, S. K. *Complex Formations in Alkali $-$ Aluminium Fluoride Melts*, Diss., Univ. of Trondheim, NTH, Trondheim, Norway 1974.
6. Temkin, M. *Acta Physicochim. URSS 20* (1945) 411.
7. Phillips, N. W. F., Singleton, R. H. and Hollingshead, E. A. *J. Electrochem. Soc. 102* (1955) 690.
8. Pearson, T. G. and Waddington, J. *Discuss. Faraday Soc. 1* (1947) 307.

9. Feinleib, M. and Porter, B. *J. Electrochem. Soc.* *103* (1956) 231.
10. Mitchell, J. C. and Samis, C. S. *Trans. Metall. Soc. AIME 245* (1969) 122.
11. Wilkening, S. and Ginsberg, H. *Metall 27* (1973) 787.
12. Sterten, Å. *Electrochim. Acta 25* (1980) 1673.
13. Kvande, H. *Thermodynamics of the System NaF $-AlF_3 - Al_2O_3 - Al$*, Diss., Univ. of Trondheim, NTH, Trondheim, Norway 1979.
14. Fuseya, G. and Takeda, B. *J. Electrochem. Soc. Jpn. 27* (1959) 339.
15. Fenerty, A. and Hollingshead, E. A. *J. Electrochem. Soc. 107* (1960) 993.
16. Rolin, M. *Bull. Soc. Chim. Fr.* (1961) 1112.
17. Foster, P. A. *J. Am. Ceram. Soc. 58* (1975) 288.
18. Foster, P. A. *J. Chem. Eng. Data 9* (1964) 200.
19. Holm, J. L. *Thermodynamic Properties of Molten Cryolite and Other Fluoride Mixtures*, Diss., Univ. of Trondheim, NTH, Trondheim, Norway 1971.
20. Kummer, J. T. *Prog. Solid State Chem. 7* (1972) 141.
21. Stull, D. R. and Prophet, H. *JANAF Thermochemical Tables*, 2nd Ed., NSRDS-NBS 37, Washington 1971.
22. Chase, M. W., Curnett, J. L., McDonald, R. A. and Syverud, A. N. *JANAF Thermochemical Tables, Suppl.* 1978.
23. Dewing, E. W. *Metall. Trans. 1* (1970) 2211.
24. Dewing, E. W. *Metall. Trans. 3* (1972) 2699.
25. Dewing, E. W. *Metall. Trans. 9B* (1978) 687.
26. Grjotheim, K., Motzfeldt, K. and Rao, D. B. In Edgeworth, T. G., Ed., *Light Metals*, Proc. AIME Meeting, New York 1971, Vol. 1, p. 223.
27. Cantor, S., Hitch, B. F. and Heatherly, D. E. In Pemsler, J. P., Braunstein, J. and Nobe, K., Eds., *Molten Salts*, Proc. Int. Symp., Electrochem. Soc., Princeton, N.J. 1976, p. 417.
28. Bjørgum, A., Sterten, Å., Thonstad, J. and Tunold, R. *Electrochim. Acta. 26* (1981) 491.
29. Frank, W. B. and Foster, L. M. *J. Phys. Chem. 61* (1957) 1531.
30. Tual, A. and Rolin, M. *Electrochim. Acta 17* (1972) 2277.
31. Grjotheim, K., Matiasovsky, K., Myhre-Andersen, S. and Øye, H. A. *Electrochim. Acta 13* (1968) 91.
32. Thonstad, J. and Rolseth, S. Ref. 1, p. 186.
33. Thonstad, J. *Can. J. Chem. 43* (1965) 3429.
34. Rolseth, S. *Tilbakereaksjonen i aluminiumelektrolysen*, Diss., Univ. of Trondheim, NTH, Trondheim, Norway 1980.
35. Rolseth, S. and Thonstad, J. In Bell, G. M., Ed., *Light Metals*, Proc. AIME Meeting, Chicago 1981, p. 289.